Journal of Molecular Catalysis A: Chemical 346 (2011) 70–78

Contents lists available at ScienceDirect

Journal of Molecular Catalysis A: Chemical

journal homepage: www.elsevier.com/locate/molcata

Ruthenium-catalysed hydrogenation of esters using tripodal phosphine ligands

Martin J. Hanton[a,*], Sergey Tin[a], Brian J. Boardman[a], Philip Miller[b]

[a] Sasol Technology UK, Purdie Building, North Haugh, St. Andrews, Fife, KY16 9ST, UK
[b] Department of Chemistry, Imperial College London, South Kensington, London, SW7 2AZ, UK

ARTICLE INFO

Article history:
Received 22 February 2010
Received in revised form 20 June 2011
Accepted 22 June 2011
Available online 29 June 2011

Key words:
Ruthenium
Phosphine
Hydrogenation
Ester
Tripodal

ABSTRACT

The synthesis of a new tripodal phosphine ligand, $N(CH_2PEt_2)_3$, N-TriPhos^{Et} is reported, and the use of tripodal ligands of this type, $N(CH_2PR_2)_3$ (R = Ph, Et), in conjunction with ruthenium for the catalysed hydrogenation of dimethyl oxalate (DMO) is reported and contrasted with catalysis using the $MeC(CH_2PPh_2)_3$ (TriPhos^{Ph}) ligand. A different order of reaction with respect to the DMO substrate is found, and the rate is slower. A study of the kinetics and mechanism of the hydrogenation of DMO with $Ru(acac)_3$/TriPhos^{Ph} is described, along with the effect of different additives to the system. The performance of $Ru(acac)_3$/TriPhos^{Ph}/Zn system with unactivated ester substrates is probed and found to proceed significantly slower. Finally, based upon experimental observations, a mechanism is proposed for ester hydrogenation using ruthenium catalysts with tripodal phosphine ligands.

1. Introduction

The reduction of carboxylic acid esters to alcohols is an important and widely used laboratory scale organic transformation that usually requires stoichiometric amounts of metal hydride reducing agents such as $LiAlH_4$ [1]. On an industrial scale however, such methods of reduction are undesirable from safety, economic and environmental perspectives; thus the catalytic reduction of esters to alcohols using dihydrogen is a much more attractive method [2,3]. Indeed, such a conversion is of no small importance being utilised for the production of fatty alcohols for surfactant applications [2,3] and being a potential route to ethane-1,2-diol from dimethyl oxalate [3,4]. At present, all commercial ester hydrogenation processes employ heterogeneous catalysts, which were typically operated at elevated pressures and temperatures ($p(H_2) > 200$ bar, $T > 100\,^{\circ}C$) [2,3], although recent developments have served to ameliorate these harsh conditions [2,5]. Nonetheless, a significant interest exists in developing homogeneous catalysts capable of this transformation, as they offer the potential for further reductions in operating conditions, and also the potential to develop selective catalysts for specific applications.

Relatively few homogeneous ester hydrogenation catalysts are known, and this paucity is testament to the difficulty of effecting this transformation [6–19]. The majority of examples have featured phosphine ligands, with electron rich trialkylphosphines showing promise, whilst facially capping tripodal phosphine scaffolds are the most effective [12,13]. However, these systems are limited to activated esters, dimethyl oxalate (DMO) being the commonly studied substrate (Scheme 1). The TriPhos^{Ph} ligand (Fig. 1, **1**) in combination with ruthenium allows hydrogenation of DMO to ethane-1,2-diol (ED) at 80 bar H_2 and 100 °C [12,13,20]. A notable example not based upon phosphines is the TriSulf^{Bu} ligand (Figs. 1 and 2), which combines facial capping coordination with electron-releasing character, and allows selective hydrogenation of DMO to methyl glycolate (MG), something not possible with existing heterogeneous catalysts [20].

Two recent reports however have demonstrated homogeneously catalysed hydrogenation of unactivated esters for the first time with reasonable rates and conversions [21,22]. Saudan et al. [21] reported mixed P/N ligand systems (Figs. 3–5) capable of reducing a range of unactivated esters with good rates and conversions at 50 bar H_2 and 100 °C, although 5–10 mol% NaOMe was required as additive. These catalyst systems also demonstrated the selectivity achievable with homogeneous catalysts, unsaturated esters being selectively hydrogenated to the unsaturated alcohols [21]. In contrast, Milstein et al. [22] described reduction of unactivated esters at only 5.3 bar H_2 and 115 °C, without the need for additives, using a ruthenium catalyst incorporating a meridional tridentate PNN ligand (Figs. 1 and 5) with an electron rich dialkylphosphanyl moiety.

An examination of these known systems suggests that electron rich phosphine moieties are a desirable characteristic of any ligand for ester hydrogenation, suggesting that the TriPhos^{Ph} ligand (**1**) which features diphenylphosphanyl moieties could be improved in this regard. However, the synthesis of tripodal phosphine ligands with dialkylphosphanyl moieties is most challenging. Hence,

* Corresponding author. Tel.: +44 0 1334 460 830; fax: +44 0 1334 460 939.
E-mail address: martin.hanton@eu.sasol.com (M.J. Hanton).

1381-1169/$ – see front matter © 2011 Elsevier B.V. All rights reserved.
doi:10.1016/j.molcata.2011.06.010

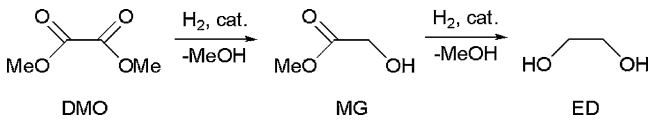

Scheme 1. The hydrogenation pathway of dimethyl oxalate (DMO).

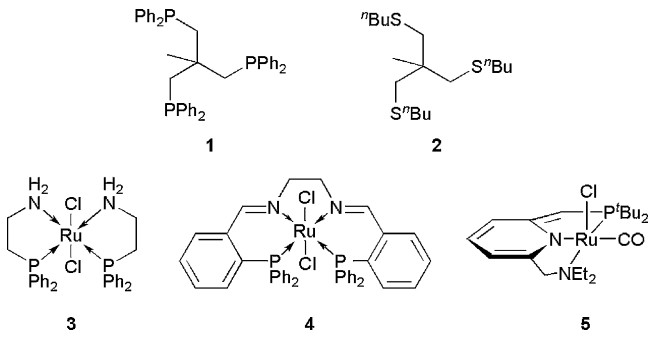

Fig. 1. Active catalysts for ester hydrogenation to alcohols: **1**, *in situ* TriPhos^{Ph} and Ru(acac)$_3$; **2**, *in situ* TriSulf^{Bu} and Ru(acac)$_3$; **3**+**4**, NP Ru catalysts developed by Saudan; **5**, PNN Ru catalyst developed by Milstein.

to date, few alkyl TriPhos derivatives have appeared in the literature even though they may be attractive for transition metal complex formation and catalysis [23–25]. Furthermore, recent work suggests that mixed P/N donor ligands offer clear benefits in terms of performance, but some of these ligands also involve convoluted syntheses.

Inspired by these observations we chose to examine ligands of the N-TriPhos scaffold (Fig. 2). These have obvious similarities

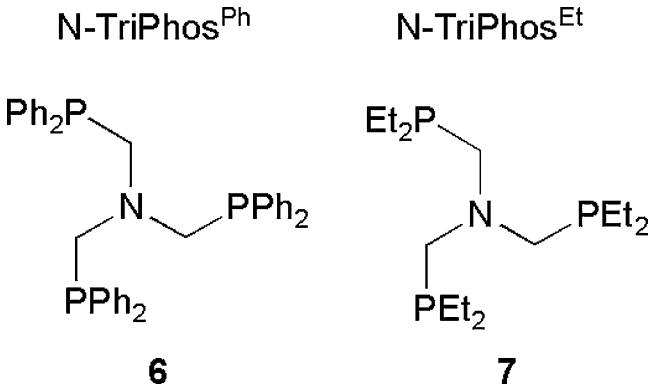

Fig. 2. The N-TriPhos ligands and complexes utilised herein.

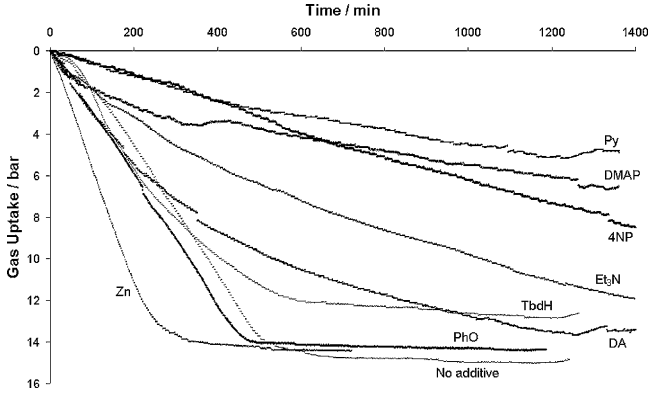

Fig. 3. Hydrogen uptake curves measured during catalysis with Ru(acac)$_3$/TriPhos^{Ph} and various additives.

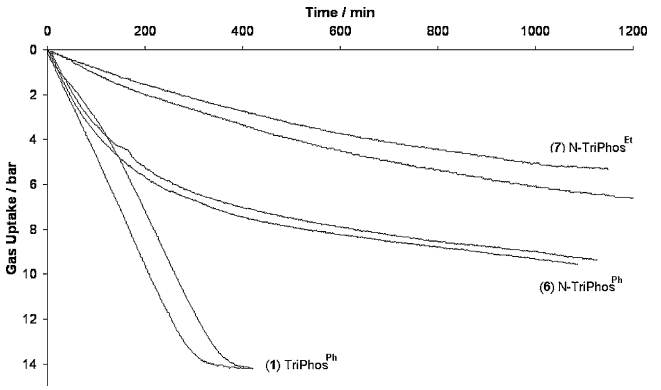

Fig. 4. Hydrogen uptake measured during catalysis with Ru(acac)$_3$ and N-TriPhos^{Ph} or TriPhos^{Ph}.

to the TriPhos framework differing only at the bridgehead of the molecule where a nitrogen atom is present instead of a C–CH$_3$ group. As facially capping tripods incorporating an amine moiety, they appear of potential interest for ester hydrogenation. Furthermore, they are prepared in a one-pot, single step reaction and allow facile incorporation of dialkylphosphanyl moieties with high yields. Two variants of the N-TriPhos ligand were selected for investigation; the known N-TriPhos^{Ph} ligand (Figs. 2 and 6) and the new N-TriPhos^{Et} ligand (Figs. 2 and 7) featuring diethylphosphanyl moieties, which it was envisaged would enhance the electron density at the ruthenium metal centre. This should accelerate oxidative addition processes, and enhance the hydridic nature of the ruthenium–hydride moiety increasing reactivity towards the

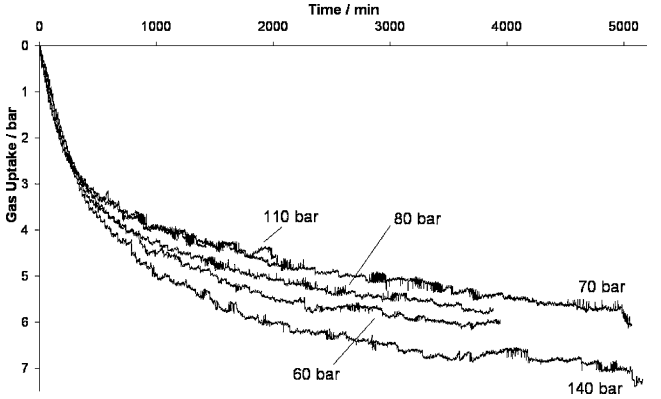

Fig. 5. Hydrogen uptake measured during catalysis with Ru(acac)$_3$ and N-TriPhos^{Ph} with varying pressure.

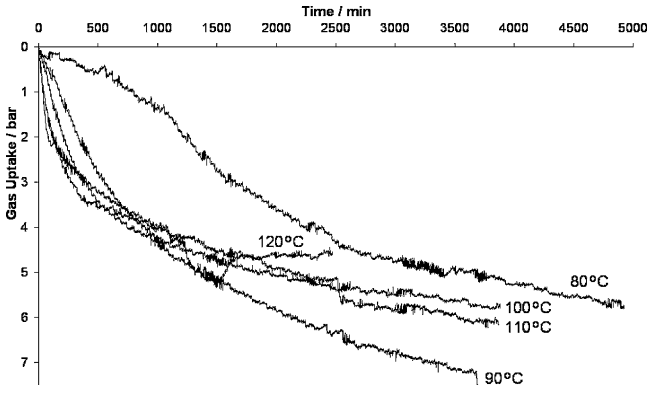

Fig. 6. Hydrogen uptake measured during catalysis with Ru(acac)$_3$ and N-TriPhos^{Ph} with varying temperature.

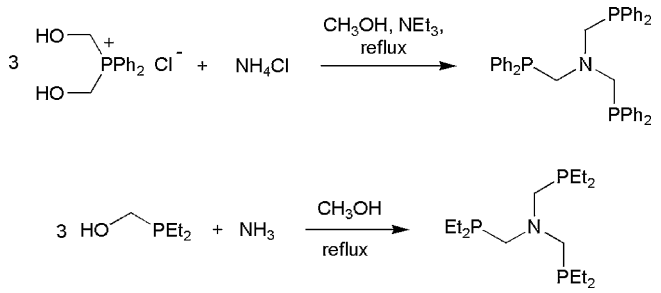

Scheme 2. Synthesis of N-TriPhos^{Ph} and N-TriPhos^{Et} ligands *via* the phosphorus based Mannich condensation reaction.

carbonyl functionality of the ester group [12]. Herein, we wish to report the use of N-TriPhos ligands for the ruthenium-catalysed hydrogenation of dimethyl oxalate and draw comparisons with the TriPhos-based system.

The use of the TriPhos^{Ph} ligand for the hydrogenation of DMO through to ED is well known, but the kinetics of this system has not previously been documented in any detail [12–15,20]. However, the kinetics by which a system operates are of interest due to the insight they may provide into the mechanism of operation of the catalyst. In a previous communication we revealed that when the Ru(acac)$_3$/TriPhos^{Ph}/Zn system was used to hydrogenate DMO, a reaction which is zero order in substrate is found [20]. Herein, we report further studies with the Ru(acac)$_3$/TriPhos^{Ph} system examining in more detail the kinetics of the DMO hydrogenation reaction and the pathway by which it proceeds; the effect of additives on this transformation and the performance of the catalyst with different substrates are also reported.

2. Results and discussion

2.1. Ligand synthesis

N-TriPhos^{Ph} was prepared as previously reported [26] following a modified procedure to that described by Markl and Jin [27]. The bis(hydroxymethyl)diphenylphosphonium chloride [28] was found to be a convenient starting material for the preparation of N-TriPhos^{Ph}. Deprotonation of this phosphonium salt *in situ* using excess triethylamine gave the corresponding hydroxymethylphosphine which was reacted with ammonium hydrochloride *via* a phosphorus based Mannich condensation reaction [29–31] (Scheme 2). N-TriPhos^{Et} was prepared directly by reaction of diethylphosphine with one equivalent of formaldehyde to generate diethylhydroxymethylphosphine which was then immediately reacted with a methanolic solution of ammonia. After 2 h at reflux the ligand separated from the methanol solution and was isolated as a viscous colourless liquid in high yield. The ^{31}P $\{^1$H$\}$ NMR spectrum of N-TriPhos^{Et} showed a single resonance at −33.2 ppm, with the ^{1}H and ^{13}C $\{^1$H$\}$ spectra being consistent with the ligand architecture.

Table 2
Composition of samples taken during a DMO hydrogenation.

Entry	Time (h)	DMO (%)	MG (%)	ED (%)
1	4	80.6	19.4	0
2	24	11.7	23.9	64.4
3	27	4.5	9.4	86.1

2.2. Catalysis

A number of reactions were performed using the Ru(acac)$_3$/TriPhos^{Ph} system to determine reproducibility [32]. As can be seen from the data in Table 1 and the graph in Fig. 3 the rate of reaction was very consistent and is clearly zero order in substrate [33], both with and without Zn as additive (entries 1–4). The reduced induction period and rate acceleration provided by zinc is clear (entry 4). The induction period is the time between the reactor vessel achieving the operating conditions of 80 bar H_2 and 100 °C, and the onset of gas uptake occurring, and is commonly observed for this type of catalysis. Triethylamine has previously been employed as an additive with the Ru(acac)$_3$/TriPhos^{Ph} system with dimethyl phthalate as substrate, on this occasion providing enhanced performance [14]. However, as can be seen from Table 1, entry 5 in the case of DMO hydrogenation a marked detrimental effect is noted for rate, but the induction period is reduced. This suggests that the additive may in fact be substrate-dependent rather than catalyst dependent. This statement is supported by the observation that zinc, which enhances DMO hydrogenation, was detrimental when the substrate was dimethyl phthalate [14]. This also raises questions about the mode of operation of the different additives, zinc having been suggested to act by enhancing the reduction of the Ru(III) precursor to Ru(II) [12]. This mode of operation would be expected to yield the reduced induction period which is observed, but does not explain the enhancement or retardation of rate depending upon substrate. This then implies that zinc at least, also affects catalysis *via* a second pathway which involves interaction with the substrate; a possible explanation being Lewis acid type interaction with the oxygen of the carbonyl group of the ester functionality leading to its activation towards reduction.

A number of other amine additives were also screened (entries 6–8: pyridine, Py; 1,5,7-triazabicyclo[4.4.0]dec-5-ene, TbdH; 4-(dimethylamino)pyridine, DMAP) but these also demonstrated a

Table 1
Results of DMO hydrogenation with Ru(acac)$_3$/TriPhos^{Ph} and various additives.

Entry	Additive	Induction period (min)	Run time (h)	Conversion (%)	TON[a]	TOF[b]	Rxn order	k[c]
1	None	160	9.4	100 (ED)	200	24.6	0	0.174
2	None	135	10.3	100 (ED)	200	25.6	0	0.181
3	None	160	10.1	100 (ED)	200	24.8	0	0.175
4	Zn (0.3%)	30	5.7	100 (ED)	200	50.3	0	0.355
5	Et_3N (10%)	50	30	93.6 (ED), 5.2 (MG)	192	7.1	0	0.050
6	Py (25%)	110	28	38.7 (MG)	39	1.7	0	0.012
7	TbdH (25%)	120	23	100 (MG)	100	11.1	0	0.079
8	DMAP (25%)	55	24	64.5 (MG)	65	1.9	0	0.014
9	PhOH (25%)	80	8.5	100 (ED)	200	25.8	0	0.182
10	4NP (25%)	10	30	40.7 (ED), 28.8 (MG)	110	4.8	0	0.034
11	DAE (25%)	25	27	98.1 (ED), 1.9 (MG)	198	6.9	0	0.049

General conditions: Ru(acac)$_3$ (212 μmol); TriPhos^{Ph} (276 μmol); DMO substrate (21.2 mmol); additive (mol% of DMO); MeOH (30 mL), $p(H_2)$ 80 bar; T 100 °C.
[a] TON determined from % conversion of DMO as determined by response factor corrected GC–MS (mol ester moiety) (mol Ru)$^{-1}$.
[b] TOF derived from rate constant (mol ester moiety) (mol Ru)$^{-1}$ h^{-1}.
[c] k = mol dm^{-3} h^{-1}.

retardation of rate with DMO as substrate. The use of fluorinated alcohols has also been demonstrated to accelerate the rate of ester hydrogenation, the mode of operation being ascribed to ionic hydrogenation due to the low pK_a of the additive rather than transesterification to yield an activated ester [14]. However, the use of fluorinated alcohols is not industrially desirable and thus we chose to examine the use of phenol (entry 9; pK_a = 9.99), but this appeared to have no effect upon rate. Thus seeking a lower pK_a additive, 4-nitrophenol (4NP) was screened (entry 10; pK_a = 7.15). However, this instead displayed inhibition, presumably due to interaction of the nitro-group with the ruthenium centre. Finally, the aminoalcohol 2-(diisopropylamino)ethanol (DAE) was examined and again rate retardation was observed. It is noteworthy that for all additives tested, the order of reaction in DMO remained zero order and induction period was always truncated, whilst the rate was influenced quite variably. This again highlights that such additives most probably act in two distinct ways; to assist in the initial formation of the catalytically active species, a mode which should be substrate independent and also to influence the rate of catalysis, which appears to be substrate dependent.

One observation of note, is that in literature reports from Matteoli and Bianchi [7–9], of DMO hydrogenation using catalysts with monodentate phosphines whilst hydrogenation occurs through MG to ED (see Scheme 1), it does do so in two distinct and separate regimes. The first regime is a 'fast' hydrogenation of DMO to MG, the second regime, being the conversion of MG to ED at a significantly slower rate, which only becomes significant once all of the DMO has been consumed. However, as can be clearly seen from Fig. 3 with TriPhos^{Ph} a different situation is observed, namely a single regime with zero order kinetics. This observation of a single 'apparent' rate implies that the Ru(acac)$_3$/TriPhos^{Ph} catalyst has a similar or greater propensity towards MG hydrogenation as compared to DMO, and when sampling is performed during a reaction both ED and MG are observed whilst unreacted DMO still remains (see Table 2). Thus a run was undertaken using MG as the substrate (with same loading of ester moiety as a DMO run, Table 3, entry 3), a zero order rate of approximately twice that for DMO being observed (0.667 versus 0.355), confirming this hypothesis. Thus it would appear that with the Ru(acac)$_3$/TriPhos^{Ph} catalyst, a juxtaposition exists compared to the case with monodentate phosphines regarding the relative rate of the two steps.

It was of interest to further probe DMO hydrogenation, and thus a reaction was undertaken with a catalyst loading of 0.025% (Table 3, entry 2) as compared to the normal 1%. It can be seen that a longer than normal induction period was observed and the rate was much slower than normal; nonetheless a turnover number of almost 1500 was achieved. Having found that this catalyst was capable of hydrogenating MG faster than DMO, we undertook to explore its potential with other substrates. The unactivated C_1, C_8 and C_{16} methyl esters, methyl acetate (Table 3, entry 4), methyl octanoate (entry 5) and methyl hexadecanoate (entry 6) were examined next. Unsurprisingly, all showed very low conversions and rates, along with extended induction periods. This again highlights the paradigm shift in performance achieved by the catalysts of Saudan and Milstein. It should be noted that the use of fluorinated alcohol additives with the Ru(acac)$_3$/TriPhos^{Ph} system has been shown to allow hydrogenation of methyl hexadecanoate [14], but as already stated such fluorine-containing additives are commercially undesirable.

Table 4
Composition of samples taken during an octanoic acid hydrogenation.

Entry	Time (h)	C_8 acid (%)	C_8 ester (%)	C_8 alcohol (%)
1	6	95.1	4.9	0
2	24	90.3	9.7	0
3	48	62.5	36.2	0.3

One particular issue of industrial concern with the hydrogenation of esters is a tolerance of carboxylic acid impurities. Many of the heterogeneous technologies suffer catalyst leaching problems due to such impurities, and so a homogeneous alternative that could tolerate these would be advantageous. Furthermore, some natural plant-derived feedstocks are converted from the carboxylic acids to esters in order to be hydrogenated, and thus a catalyst that could hydrogenate the carboxylic acid directly would also be desirable. To investigate inhibition by carboxylic acids, a DMO hydrogenation was performed that was spiked with 10% glycolic acid relative to DMO (Table 3, entry 7). As can be seen catalysis proceeded comparatively smoothly; a slightly increased induction period was observed and the rate was halved, but total conversion to ED was achieved. Notably, no trace of glycolic acid was detected by GC–MS, and by comparison with standards it was determined that this material had been converted to ED. In a separate experiment, glycolic acid was stirred in MeOH at 60 °C and was readily esterified to MG, suggesting that the glycolic acid is not hydrogenated directly, but following esterification under these conditions. Finally, an attempt was made to hydrogenate octanoic acid directly (Table 3, entry 8); subsequent analysis revealed only trace reduction to octanol, but at a level only slightly lower than when methyl octanoate was employed. However, significant esterification of the substrate to methyl octanoate did occur and again suggests that the acid is perhaps not hydrogenated directly; certainly, from samples taken during catalysis (see Table 4), no trace of octanol is observed until a significant concentration of methyl octanoate has formed.

Having explored the potential and limitations of the TriPhos^{Ph} ligand system, and noting the improvements offered by the ligand systems of Saudan and Milstein, we decided to explore tripodal

Table 3
Hydrogenation of differing ester substrates with Ru(acac)$_3$/TriPhos^{Ph}.

Entry	Substrate	Induction period (min)	Run time (h)	Conversion (%)	TON[a]	TOF[b]	Rxn order	k[c]
1	DMO	30	5.7	100 (ED)	200	50.3	0	0.355
2	DMO[d]	250	125	36.4 (MG)	1456	16.6	0	0.012
3	MG[e]	30	4.9	100 (ED)	200	94.4	0	0.667
4	MA	200	96	24.7 (EtOH)	24.7	2.3	0	0.017
5	C_8 ester	160	22	3.1 (C_8OH)	0.4	–	0	0.002
6	C_{16} ester	180	22	0.8 (C_{16}OH)	0.1	–	0	–
7	DMO/GA	60	12	100 (ED)	210	19.0	0	0.134
8	C_8 acid	190	49	0.3 (C_8OH)	0.3	–	0	–

General conditions: Ru(acac)$_3$ (212 μmol); TriPhos^{Ph} (276 μmol); substrate (21.2 mmol); Zn (63.6 μmol); MeOH (30 mL), $p(H_2)$ 80 bar; T 100 °C.
[a] TON determined from % conversion of DMO as determined by response factor corrected GC–MS (mol ester moiety) (mol Ru)$^{-1}$.
[b] TOF derived from rate constant (mol ester moiety) (mol Ru)$^{-1}$ h^{-1}.
[c] k = mol dm^{-3} h^{-1}.
[d] Ester moiety (85.2 mmol); Ru(acac)$_3$ (21.3 μmol).
[e] Substrate (42.4 mmol).

Table 5
Results of DMO hydrogenation with various tripodal phosphine ligands.

Entry	Ligand	Induction Period (min)	Run Time (h)	Conv. (%)	TON[a]	TOF[b]	Rxn Order	k[c]
1	TriPhos^{Ph}	10	7	98.5 (ED)	197.0	36.8	0	0.260
2	TriPhos^{Ph}	10	7	98.6 (ED)	197.2	39.3	0	0.278
3	N-TriPhos^{Ph}	153	20.5	95.7 (MG)	95.7	2.0	1	0.014
4	N-TriPhos^{Ph}	143	20.9	96.6 (MG)	96.6	2.2	1	0.016
5	N-TriPhos^{Et}	249	20.3	7.8 (ED), 74.7 (MG)	90.3	4.7	1	0.033
6	N-TriPhos^{Et}	169	20.6	5.6 (ED), 93.0 (MG)	104.2	5.3	1	0.037

General conditions: $Ru(acac)_3$ (212 μmol); ligand (276 μmol); DMO (21.2 mmol); Zn (63.6 μmol); MeOH (30 mL); $p(H_2)$ 80 bar; T 100 °C.
[a] TON determined from % conversion of DMO as determined by response factor corrected GC–MS (mol ester moiety) (mol Ru)$^{-1}$.
[b] TOF derived from rate constant (mol ester moiety) (mol Ru)$^{-1}$ h^{-1}.
[c] k = zero-order k in mol dm^{-3} h^{-1} and first-order k in s^{-1}.

Table 6
Results of DMO hydrogenation with $Ru(acac)_3$/N-TriPhos^{Ph} with varying pressure.

Entry	Pressure (bar)	Induction period (min)	Run time (h)	Conv. (%)	TON[a]	TOF[b]	Rxn order	$k \times 10^3$[c]
1	60	236	66	64.1 (ED), 35.9 (MG)	164.1	0.9	1	3.2
2	70	291	84	41.8 (ED), 58.2 (MG)	141.8	0.6	1	2.0
3	80	217	66	53.5 (ED), 46.5 (MG)	153.5	0.7	1	2.4
4	110	333	34	2.7 (ED), 97.3 (MG)	102.7	0.8	1	2.9
5	140	234	86	19.8 (ED), 80.2 (MG)	119.8	0.4	1	1.3

General conditions: $Ru(acac)_3$ (106 μmol); ligand (137.8 μmol); DMO (10.6 mmol); Zn (31.8 μmol); MeOH (30 mL); T 100 °C.
[a] TON determined from % conversion of DMO as determined by response factor corrected FID–GC (mol ester moiety) (mol Ru)$^{-1}$.
[b] TOF derived from rate constant (mol ester moiety) (mol Ru)$^{-1}$ h^{-1}.
[c] k = first-order k in s^{-1}.

phosphine ligands incorporating an additional nitrogen moiety albeit in the ligand backbone rather than as a donor atom, due to the ease of synthesis. Table 5 summarises the data from initial catalytic studies with the N-TriPhos^{Ph} (**6**) and N-TriPhos^{Et} (**7**) ligands for DMO reduction, and includes runs with the TriPhos^{Ph} ligand conducted at the same time for accurate comparison. A graphic representation of the gas uptake during this catalysis can be seen in Fig. 4. Given that zinc was the only additive to show a beneficial effect with the TriPhos^{Ph} ligand, it was used consistently in the studies with the N-TriPhos ligands, and no other additives were examined.

As can be seen, both variants of the N-TriPhos ligand gave longer induction times than the benchmark system and much slower conversion of the substrate, but the most significant difference was the different order of reaction in substrate, which appears to be first order based upon a plot of $\ln([DMO]/[DMO]_o)$. The mechanistic implication of this, is that either the binding of DMO is the rate determining step in catalysis with N-TriPhos or that a Ru–DMO complex is involved in the rate determining step and the concentration of this species is in turn dependant upon the rate of DMO binding. This situation is in contrast to that with TriPhos^{Ph}.

In order to further explore catalysis with the N-TriPhos^{Ph} ligand, studies of the influence of pressure (Table 6 and Fig. 5) and temperature (Table 7 and Fig. 6) upon reaction were undertaken. These studies reveal that over the pressure regime examined (60–140 bar) there is apparently no dependency upon the hydrogen pressure, suggesting that oxidative addition of hydrogen to ruthenium is not involved in the rate determining step. This is consistent with the observation that the reaction is first-order in DMO, suggesting this is involved in the rate determining step (*vide supra*). Concerning the effect of temperature, whilst the reaction at 80 °C was markedly slow, there was no apparent increase in rate upon moving from 90 to 120 °C in 10 °C steps. This is curious and could be explained through catalyst decomposition (*vide infra*) increasing with temperature and off-setting the rate enhancement expected from increased thermal energy.

It should be noted that whilst a plot of $\ln([DMO]/[DMO]_o)$ versus time for catalysis with the N-TriPhos^{Et} ligand was linear over the entire reaction period, for reactions with the N-TriPhos^{Ph} ligand (Tables 5–7) a significant deviation from linearity is observed during the first part of reaction. Hence, for the catalytic data with the N-TriPhos^{Ph} ligand the rate was calculated using only the data that conformed to linearity. With regards to what is occurring during this first period of the catalysis, sampling of the reaction reveals that no conversion of DMO is apparent despite the consumption of hydrogen. Based upon sampling studies, the onset of DMO hydrogenation appears to roughly correlate with the point at which a plot of $\ln([DMO]/[DMO]_o)$ versus time becomes linear. Analysis of samples taken during reaction also reveals that in contrast to catalysis with the TriPhos^{Ph} ligand, the formation of ED does not appear to occur until most of the DMO has been hydrogenated to MG. In order to probe whether the unexplained initial hydrogen consumption was due to over hydrogenation of the DMO to ethane or even methane, the gas headspace of a reaction was sampled and screened

Table 7
Results of DMO hydrogenation with $Ru(acac)_3$/N-TriPhos^{Ph} with varying temperature.

Entry	Temp. (°C)	Induction period (min)	Run time (h)	Conv. (%)	TON[a]	TOF[b]	Rxn order	$k \times 10^3$[c]
1	80	236	82	18.1 (ED), 80.9 (MG)	117.0	0.6	1	2.3
2	90	291	61	53.1 (ED), 46.9 (MG)	153.1	1.3	1	4.5
3	100	217	66	53.5 (ED), 46.5 (MG)	153.5	0.7	1	2.4
4	110	333	64	40.0 (ED), 60.0 (MG)	140.0	1.1	1	3.8
5	120	234	41	41.8 (ED), 58.2 (MG)	141.8	1.7	1	6.1

General conditions: $Ru(acac)_3$ (106 μmol); ligand (137.8 μmol); DMO (10.6 mmol); Zn (31.8 μmol); MeOH (30 mL); $p(H_2)$ 80 bar.
[a] TON determined from % conversion of DMO as determined by response factor corrected FID–GC (mol ester moiety) (mol Ru)$^{-1}$.
[b] TOF derived from rate constant (mol ester moiety) (mol Ru)$^{-1}$ h^{-1}.
[c] k = first-order k in s^{-1}.

Table 8
Results of DMO hydrogenation with Ru(N-TriPhos^{Ph})$(CO)_2$ with varying additives.

Entry	Additive (°C)	Amount of additive (eq. to Ru)	Run time (h)	Conv. (%)	TON[a]	TOF[b]	Rxn order	$k \times 10^{3}$[c]
1	None	–	119	–				
2	Zn	0.3	38	–				
3	Water	10.5	80	–				
4	Me_3NO	3	158	44.1 (MG)	44.1	0.7	1	2.6
5	AgI	3	89	–				

General conditions: $Ru(acac)_3$ (106 μmol); ligand (137.8 μmol); DMO (10.6 mmol); Zn (31.8 μmol); MeOH (30 mL); $p(H_2)$ 80 bar.
[a] TON determined from % conversion of DMO as determined by response factor corrected FID–GC (mol ester moiety) (mol Ru)$^{-1}$.
[b] TOF derived from rate constant (mol ester moiety) (mol Ru)$^{-1}$ h^{-1}.
[c] k = first-order k in s^{-1}.

by TCD–GC. Only hydrogen and traces of argon were detected, no ethane or methane being present (the lower limit for detection of these hydrocarbons was 5 ppm). This sample was also examined for CO_2 (lower detection limit 20 ppm) as this is another possible decomposition pathway for DMO, but again none was detected. As another method of checking for hydrogenative decomposition of the DMO during this initial phase, two reactions were conducted in the presence of internal standards (one with nonane and one with 2,6-dimethylphenol), but this again confirmed that no substrate was 'disappearing', the total moles of DMO, MG and ED remaining constant between the start and end of reaction. Hence, to date this initial non-productive hydrogen consumption remains without good explanation.

Given the decreased rate with N-TriPhos^{Ph} compared to TriPhos^{Ph}, the apparent change in kinetic profile during reaction and the observation that increased temperature does not increase rate (*vide supra*), several reactions were sampled at the end and examined for signs of ligand decomposition by $^{31}P\{^1H\}$ NMR spectroscopy and GC–MS. The $^{31}P\{^1H\}$ NMR spectroscopy revealed that the single peak for the N-TriPhos^{Ph} ligand at δ-28.9 was completed replaced by a number of peaks between δ20 and 40, which are believed to correspond to the phosphine oxides, based upon comparison with an authentic sample of ligand left open to air for one week. A small peak was also detected which corresponded to Ph_2PH, and this species was also identified by the GC–MS analysis. This strongly suggests that the N-TriPhos^{Ph} ligand does suffer extensive decomposition under reaction conditions. In contrast, similar studies with the TriPhos^{Ph} ligand revealed that at the end of reaction most ligand remained unoxidised.

Finally, in order to probe if catalysis with the N-TriPhos^{Ph} ligand could be enhanced using a pre-formed ruthenium complex, Ru(N-TriPhos^{Ph})$(CO)_2$ (**8**), was prepared by the reaction of N-TriPhos^{Ph} with $[Ru_3(CO)_{12}]$ in toluene. The $^{31}P\{^1H\}$ NMR spectrum showed a single resonance at 8.3 ppm indicating coordination of all three phosphorus and forming the expected facial capping geometry of the N-TriPhos^{Ph} ligand to the Ru centre. This complex was examined in the hydrogenation of DMO. The results obtained are summarised in Table 8 and reveal that this strategy was not successful. Use of this complex with or without zinc as additive did not lead to any hydrogenation of DMO, and it was speculated that this was due to the ruthenium having an oxidation state of zero, whilst the active species is theorised to be ruthenium(II) (*vide infra*). Hence, the use of the potentially oxidising additives, water, trimethylamine oxide and silver iodide, was probed. Unfortunately, only the use of trimethylamine oxide gave any catalysis and at a rate inferior to that with the *in situ* system ($Ru(acac)_3$ + N-TriPhos^{Ph}). However, this does support the hypothesis that oxidation of the ruthenium centre is required for catalysis if ruthenium (0) is used as a pre-catalyst.

Finally, we propose a mechanistic pathway by which reaction may proceed with catalysts of this type (Fig. 7). The first step is formation of the active species, and it is this believed to account for the induction period observed. Hydrogenative loss of the 2,4-pentanedionate (acac) ligands from the ruthenium centre is suggested, with concomitant binding of the tripodal phosphine to leave a ruthenium (II) species, there being an overall net reduction from ruthenium (III). Certainly, the hydrogenative loss of the acac ligands is substantiated by the observation in the GC analysis of trace amounts of 2,4-pentanediol in all the catalysis performed herein. Thus, the initial catalyst species is shown as a 16 electron ruthenium dihydride stabilised by the TriPhos^{Ph} ligand, but in reality may well exist with solvent or dihydrogen bound as an 18 electron species. The first step is binding of the DMO to the ruthenium *via* the ester carbonyl function. The zero-order dependence on substrate observed for the TriPhos^{Ph} ligand suggests that in this scenario, the DMO binding is facile. However, given the first order dependence on substrate observed for the N-TriPhos ligand, this initial binding of the DMO is suggested to be the rate limiting step. Nonetheless, after binding of the DMO, the resultant species then undergoes an insertion of the carbonyl moiety into the metal hydride bond to give an alkoxide, which would be expected to readily form a four-membered OÔ chelate regenerating an 18 electron complex [34,35]. Reductive elimination of the alkoxide would yield a hemiacetal, which are well known to spontaneously rearrange to yield the aldehyde [35]. The 14 electron ruthenium (0) TriPhos^{Ph} species would be expected to readily add hydrogen to regenerate the initial catalyst species (TriPhos^{Ph})$Ru^{II}(H)_2$ [36]. The hydrogenation of the aldehyde species *via* coordination, insertion and reductive elimination steps is generally considered to be facile as compared to the hydrogenation of the ester carbonyl, and yields the product alcohol, regenerating the same 14 electron ruthenium (0) species.

The ability of tripodal phosphine ligands to stabilise the electron deficient 14-electron ruthenium (0) species is suggested to be a crucial property, and may explain why many ligands do not produce stable catalysts, the ruthenium metal being lost as ruthenium (0), most probably at this stage. Furthermore, the electron donating phosphine ligand should facilitate the oxidative addition of dihydrogen to the ruthenium at this stage to regenerate (tripodal phosphine)$Ru^{II}(H)_2$. Whilst the success of tripodal phosphine ligands are believed to stem in part from the rationale above, a further consideration maybe the regiochemistry of the ligand coordination. All three of the coordination sites not occupied by the ligand are mutually *cis* – facilitating the transformations that occur at the metal centre [37]. Whilst these transformations are not precluded with a meridional arrangement of ancillary ligand(s), the existence of *trans*-coordination sites means rearrangement of the ligands at the metal centre may need to occur before reaction can occur, whereas with a facial arrangement of coordination sites, even after an insertion, the resulting hydride and alkyl will be situated in a *cis*-fashion ready to undergo reductive elimination.

In the mechanism proposed herein, only a single ester molecule is shown interacting with the ruthenium centre at any time, on

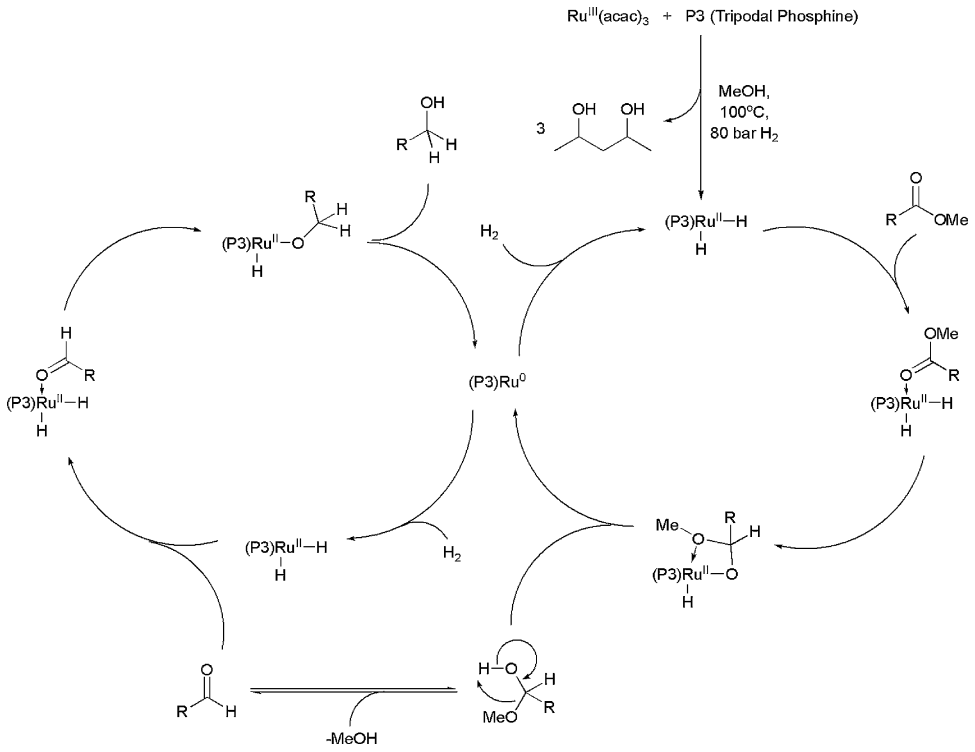

Fig. 7. Proposed mechanism of DMO hydrogenation with tripodal phosphine ligands.

the basis of steric congestion and coordinative saturation whilst the ester is bound. However, the possibility of the interaction of a second ester molecule cannot be ruled out. At the points when coordinative unsaturation does formally occur, for example the $(P3)Ru^0$ and $(P3)Ru^{II}(H)_2$ intermediates, it is quite possible that these species never really exist and solvent is bound or another ester molecule is almost immediately coordinated (certainly in the case of TriPhos^{Ph} where the DMO is not involved in the rate determining step). Indeed, the inhibiting effect of the amine additives could well be explained by their coordination to these species, which subsequently preclude binding of the ester substrate.

3. Conclusions

The pathway of dimethyl oxalate hydrogenation with the Ru(acac)$_3$/TriPhos^{Ph} catalyst system has been shown to involve a slow initial reduction of dimethyl oxalate to methyl glycolate, followed by a comparatively fast reduction of the methyl glycolate to ethane-1,2-diol, such that an overall single zero order rate in substrate is apparent. Interestingly, this situation is the reverse of that observed when monodentate phosphine systems are employed. A number of new additives have been screened in concert with the Ru(acac)$_3$/TriPhos^{Ph} catalyst, and whilst all truncate the induction period, none of the new additives tested increase the rate. The ability of this system to hydrogenate different substrates has been further explored and its inherent activity towards simple aliphatic esters is very low. However, the tolerance of the system towards carboxylic acids has been shown to be very good. Finally, we have demonstrated the first use of N-TriPhos type ligands in conjunction with ruthenium for the hydrogenation of esters, and note an interesting change in kinetics, indicative of substrate binding becoming implicated with rate determining step. However, further studies have revealed that the N-TriPhos scaffold undergoes extensive decomposition during catalysis. The use of a discreet Ru–(N-TriPhos^{Ph-}) complex for catalysis was also examined, but this did not offer any advantages over the *in situ* system.

4. Experimental

4.1. General considerations

All preparations were carried out using standard Schlenk line techniques under an inert atmosphere of N_2 unless otherwise stated. For synthesis, solvents were dried over standard drying agents and freshly distilled under nitrogen before use. All starting materials were of reagent grade, purchased from either Aldrich Chemical Company or Strem Chemicals. ^{1}H, ^{13}C $\{^1$H$\}$ and ^{31}P $\{^1$H$\}$ NMR spectra were recorded on Bruker Av-400, DRX-400 or Av-500 spectrometers. Chemical shifts are reported in ppm and referenced using the residual proton impurities in the solvents. Pneumatically assisted ESI–MS was performed using a Bruker MicrOTOF-Q II instrument equipped with Apollo II ion funnel ESI source coupled directly to an MBraun glovebox for inert injection. Prior to accurate mass determination calibrated with Agilent ESI tuning mixture over the range 50–3000 m/z was performed. The sample was analysed as a 1 μg/mL solution in dry, deoxygenated MeCN at a flow rate 3 μL/min. Instrument settings were unexceptional (capillary = 4500 V; nitrogen drying gas at 100 °C and 4 L/min flow rate).

For catalysis, Aldrich anhydrous grade methanol was sparged with dry N_2, but otherwise used as received. GC–MS analysis was performed on an Agilent Technologies 6890 N GC system equipped with MDN12 (60 m × 0.25 mm × 0.25 μm) column, coupled to an Agilent Technologies 5973 N MSD Mass Spectrometric instrument equipped with EI source.

4.2. General protocol for catalysis

A 50 mL s/s autoclave equipped with gas entraining stirrer and sampling valve, was charged with $Ru(acac)_3$, DMO, Zn and ligand, then flushed with dry N_2. Dry MeOH (30 mL) was added, and the vessel was pressurised to 80 bar with H_2 then vented, three times. The vessel was then pressurised with 60 bar H_2, heated to 100 °C and when reaction temperature was attained, the vessel pressure was topped up to 80 bar H_2. This was considered to be the starting point of reaction, an induction period normally being observed between this point and the onset of catalysis. During reaction the pressure in the vessel was maintained *via* a temperature compensated ballast vessel and the rate of catalysis was assessed by measuring the pressure drop in the ballast vessel which was logged with a polling frequency of 1 s. Samples taken during catalysis *via* the sampling valve were immediately analysed by GC–MS. When gas uptake had ceased or the reaction was deemed to have run for sufficient time, the vessel was cooled to RT, the excess pressure vented, the vessel opened to air and a sample taken for GC–MS analysis. Unless stated otherwise, a transparent solution free from any precipitate was always observed upon opening the vessel. All GC–MS data was response factor corrected based on calibration experiments with compounds of interest. For the N-TriPhos^{Et} ligand which is not air stable, the ligand was prepared as a stock solution in MeOH and added to the vessel with the solvent, once an inert atmosphere had been achieved.

4.3. N,N,N-tris(diethylphosphinomethyl)amine (**7**)

To a Schlenk flask was added diethyl phosphine (1.0 g, 11.1 mmol), methanol (5 mL) and formaldehyde solution (1.2 mL, 35% w/w) and the mixture stirred at room temperature for 3 h forming diethylhydroxymethylphosphine. To this solution was added a methanolic solution of ammonia (1.85 mL, 2 M) and the mixture brought to reflux for 2 h. After this time the ligand separated from the solvent into two distinct colourless layers. The methanol layer was conveniently removed using a cannula and the clear colourless viscous ligand was rinsed with methanol (2 mL × 5 mL) and then dried *in vacuo* overnight (1.1 g, 92%). ^{1}H NMR ($CDCl_3$, 400 MHz): δ 2.91 (s, br, 6H, CH_2), 1.45–1.39 (m, 12H, CH_2), 1.07 (dt, 18H, $^3J_{PH}$ = 14.2 Hz, $^3J_{HH}$ = 7.7 Hz). ^{13}C {^{1}H} NMR ($CDCl_3$, 100 MHz): δ 58.3 (br m, N–CH_2), 18.2 (d, $^1J_{PC}$ = 10.8 Hz, P–CH_2), 9.9 (d, $^2J_{PC}$ = 12.8 Hz, –CH_3). ^{31}P {^{1}H} NMR ($CDCl_3$, 162 MHz): δ −33.2. MS (ESI, +ve, accurate mass) *m/z*: measured 322.1974 $[M-H]^+$, expected 322.1977, error = 0.3 mDa/1.0 ppm. Anal. Calcd. for $C_{15}H_{36}NP_3$ (found): C, 55.71 (55.61); H, 11.22 (11.30); N, 4.33 (4.41).

4.4. [(N-TriPhos^{Ph})Ru(CO)$_2$] (**8**)

To mixture of N-TriPhos^{Ph} (1.0 g, 1.63 mmol) and $[Ru_3(CO)_{12}]$ (347 mg, 0.54 mmol) was added toluene (30 mL) and the mixture brought to reflux. Evolution of CO gas was clearly observed on heating the solution. After 12 h reflux, the bright orange reaction mixture which contained a small amount of metallic ruthenium was filtered *via* cannula to a new flask. The volume of solvent reduced *in vacuo* to approximately 5 mL, at which point an orange crystalline solid began to form. The mixture was then heated to dissolve the solid. An orange crystalline solid formed on cooling to room temperature. The supernatant was removed using a cannula and the crystalline solid rinsed with toluene (2 × 5 mL) and dried *in vacuo* overnight. A second batch of crystals was obtained from the combined supernatant and rinsing solutions. (Total yield = 1.09 g, 84%.) ^{1}H NMR ($CDCl_3$, 400 MHz): δ 7.42–6.87 (m, 30H), 3.93 (s, 6H, CH_2). ^{31}P {^{1}H} NMR (C_6D_6, 162 MHz): δ 8.25. FT-IR (ν/cm^{-1}): carbonyl stretches 1940 (w), 1853 (w), others 1460 (s), 1376 (s). MS (ES +ve) *m/z*: 357 $[N(CH_2PPh_2)_3Ru]^{2+}$. Anal. Calcd. for $C_{15}H_{36}NP_3$ (found): C, 63.98 (64.12); H, 4.85 (4.81); N, 1.82 (1.82).

Acknowledgements

MJH would like to thank Sasol Technology UK Ltd. and Sasol Technology (Pty) Ltd for permission to publish this work. Prof. David Cole-Hamilton, Prof. Bob Tooze and Dr. David Smith are thanked for useful discussions. The referees are thanked for some useful suggestions. PWM is grateful to the EPSRC for the award of a Life Sciences Interface fellowship (EP/E039278/1).

References

[1] J. March, Advanced Organic Chemistry: Reactions Mechanisms and Structure, 4th Ed., Wiley-Interscience, New York, 1992, pp. 1213–1215, and references therein.
[2] CEH Marketing Research Report, "Detergent Alcohols", R.F. Modler, 2004; PEP Review 93–2–1, "Natural Detergent Alcohols by a Vapour Phase Ester Hydrogenation Process", W.S. Fong, 2004.
[3] N.W. Cant, D.L. Trimm, T. Turek, Catal. Rev. Sci. Eng. 36 (1994) 645–683.
[4] CEH Product Review, "Mono-, di- and tri-ethylene glycols", J. Lacson, 2003.
[5] Davy McKee, M. Wilmott, et al., US 5,138,106 (1992).;
Davy McKee, M. Wilmott, et al., US 5,157,168 (1992).
[6] R.A. Grey, G.P. Pez, A. Wallo, J. Am. Chem. Soc. 103 (1981) 7536–7542;
R.A. Grey, G.P. Pez, J. Corsi, A. Wallo, J. Chem. Soc. Chem. Commun. (1980) 783–784;
R.A. Grey, G.P. Pez, US 4232170 (1980), Allied Chemicals;
R.A. Grey, G.P. Pez, Fundamental Research in Homogeneous Catalysis, vol. 4, 1984, pp. 97–116;
R.A. Grey, G.P. Pez, Prepr. Pap. Natl. Meet., Div. Petrol. Chem., Am. Chem. Soc. 25 (1980) 399–403.
[7] U. Matteoli, G. Menchi, M. Bianchi, F. Piacenti, P. Frediani, J. Mol. Catal. 22 (1984) 353–362;
U. Matteoli, G. Menchi, M. Bianchi, P. Frediani, F. Piacenti, J. Mol. Catal. 29 (1985) 269–270;
U. Matteoli, G. Menchi, M. Bianchi, F. Piacenti, J. Mol. Catal. 44 (1988) 347–355;
U. Matteoli, G. Menchi, M. Bianchi, F. Piacenti, S. Ianelli, M. Nardelli, J. Organomet. Chem. 498 (1995) 177–186.
[8] U. Matteoli, G. Menchi, M. Bianchi, F. Piacenti, J. Organomet. Chem. 299 (1986) 233–238.
[9] U. Matteoli, G. Menchi, M. Bianchi, F. Piacenti, J. Mol. Catal. 64 (1991) 257–267.
[10] K. Nomura, H. Ogura, Y. Imanishi, J. Mol. Catal. 166 (2001) 345–349;
K. Nomura, H. Ogura, Y. Imanishi, J. Mol. Catal. 178 (2002) 105–114.
[11] Y. Hara, H. Inagaki, S. Nishimura, K. Wada, Chem. Lett. (1992) 1983–1986.
[12] M.C. van Engelen, H.T. Teunissen, J.G. De Vries, C.J. Elsevier, J. Mol. Catal. A: Chem. 206 (2003) 185–192.
[13] H.T. Teunissen, C.J. Elsevier, Chem. Commun. (1997) 667–668.
[14] H.T. Teunissen, C.J. Elsevier, Chem. Commun. (1998) 1367–1368.
[15] M. Kilner, D.V. Tyers, S.P. Crabtree, M. A. Wood, WO 03/093208 A1 (2003), Davy Process Technology.
[16] M.L. Clarke, M. Belén Díaz-Valenzuela, A.M.Z. Slawin, Organometallics 26 (2007) 16–19.
[17] W. Kuriyama, Y. Ino, O. Ogata, N. Sayo, T. Saito, Adv. Synth. Catal. 352 (2010) 92–96.
[18] S. Takebayashi, S.H. Bergens, Organometallics 28 (2009) 2349–2351.
[19] H. Maeda, K. Inoue, T. Matsumoto, I. Nagasaki, R. Noyori, S. Saito, EP 2141142 A1, Takasago International Corp., 2010.
[20] B. Boardman, M.J. Hanton, H. van Rensburg, R.P. Tooze, Chem. Commun. (2006) 2289–2291.
[21] L.A. Saudan, C.M. Saudan, C. Debieux, P. Wyss, Angew. Chem. Int. 46 (2007) 7473–7476.
[22] J. Zhang, G. Leitus, Y. Ben-David, D. Milstein, Angew. Chem. Int. 45 (2006) 1113–1115.
[23] J.-C. Hierso, R. Amardeil, E. Bentabet, R. Broussier, B. Gautheron, P. Meunier, P. Kalck, Coord. Chem. Rev. 236 (2003) 143.
[24] H.A. Mayer, W.C. Kaska, Chem. Rev. 94 (1994) 1239.
[25] C. Bianchini, A. Meli, M. Peruzzini, F. Vizza, F. Zanobini, Coord. Chem. Rev. 120 (1992) 193.
[26] P.W. Miller, A.J.P. White, J. Organomet. Chem. 695 (2010) 1138.
[27] G. Markl, G.Y. Jin, Tetrahedron Lett. 22 (1981) 1105.
[28] J. Fawcett, P.A.T. Hoye, R.D.W. Kemmitt, D.J. Law, D.R. Russell, J. Chem. Soc. Dalton Trans. (1993) 2563.
[29] G.M. Brown, M.R.J. Elsegood, A.J. Lake, N.M. Sanchez-Ballester, M.B. Smith, T.S. Varley, K. Blann, Eur. J. Inorg. Chem. (2007) 1405.
[30] D.A. Clarke, P.W. Miller, N.J. Long, A.J.P. White, Dalton Trans. (2007) 4556.
[31] P.W. Miller, N.J. Long, A.J.P. White, Dalton Trans. (2009) 5284.
[32] A number of 'blank' reactions were also conducted to verify that no hydrogenation or DMO decomposition occurred without all components of the catalyst system present (MeOH + DMO; MeOH + DMO + Zn; MeOH + DMO + Zn + TriPhos^{Ph}; MeOH + DMO + Zn + $Ru(acac)_3$; MeOH + DMO + Ru $(acac)_3$).

[33] Rate constants were determined using GC–MS (response factor corrected) to determine the level of conversion of DMO and using this to scale the uptake of hydrogen and correlate this with [DMO]t. For zero order reactions, the rate constant was then calculated from linear regression of [DMO] versus time between the period of 20–80% feed conversion. For first order reactions, the rate constant was determined from linear regression of $\ln([DMO]_t/[DMO]_o)$ versus time between the period of 20–80% feed conversion, or the period of the reaction that gave a linear plot for these parameters.

[34] An alternative, but less probable option at the insertion stage, with both the ester and aldehyde carbonyl functions is C–O insertion (rather than O–C) to form a Ru–C bond. However, such an insertion would not be readily facilitated from a carbonyl bound in σ-donor fashion *via* the oxygen, but would require a π-bound carbonyl function to facilitate the insertion to give a Ru–C bond. Insertion with this orientation would also be sterically disfavoured. In the case of the ester substrate, at this point the Ru–C species could simply undergo a reductive elimination to yield the hemiacetal, or alternatively, loss of methanol from the 'metal bound hemiacetal' could be envisaged to yield a η^1–acyl complex. This in turn could be expected to reductively eliminate with the metal hydride to yield an aldehyde. This aldehyde maybe lost from the metal centre, although the possibility of it being retained whilst oxidative addition of dihydrogen occurs should be considered. This leads to a pathway whereby the substrate remains bound to the ruthenium throughout, and could explain the failure to observe aldehyde intermediates, both in our study and those reported in the literature.

[35] This compares with the suggestion that free aldehyde results from decomposition of the liberated hemiacetal, but is not observed due to the much greater rate of aldehyde hydrogenation compared with that for the ester [10].

[36] Indeed, under these conditions and when the binding of substrate is the rate determining step, the resting state of the catalyst may in fact be an 18 electron dihydride–hydrogen adduct species $(TriPhos^{Ph})Ru^{II}(H_2)(H)2$.

[37] Reductive elimination and insertion reactions requiring *cis*-coordination sites to proceed, and oxidative additions of non-polar species (e.g. H_2) occurring to yield *cis*-geometry species.